Supplemental Material: Neuronal Oscillations on Evolving Networks: Dynamics, Damage, Degradation, Decline, Dementia, and Death

Alain Goriely[1], Ellen Kuhl[2], and Christian Bick[3,4,1]

[1]*Mathematical Institute, University of Oxford, Oxford, UK*
[2]*Living Matter Laboratory, Stanford University, Stanford, USA*
[3]*Department of Mathematics, University of Exeter, Exeter, UK*
[4]*Institute for Advanced Studies, Technische Universität München, München, Germany*

(Dated: June 19, 2020)

S1. WEIGHTED ADJACENCY MATRIX

When weighing the adjacency matrix, we scale the adjacency matrix to model a transport process through the axon. Transport is enhanced by the number of axonal fibers $n_{ij} \in \mathbb{R}$ between two nodes and decrease with distance $l_{ij} \in \mathbb{R}_0$. The number of fibers is real in general as it is obtained as averaged over multiple data sets. For this analysis, we assume that the weights are given by $w_{ij} = n_{ij}/l_{ij}$ and the Laplacian is

$$\mathbf{L} = \rho(\mathbf{D} - \mathbf{W}), \tag{S1}$$

where $\mathbf{D}$ is the diagonal matrix with $d_{kk} = \sum_{j=1}^{N} w_{kj}$ and ρ is an overall velocity constant defining the time-scale of transport. This scaling assumes that the transport motion along the edges scales as a ballistic process. This assumption is suitable to describes nonlinear processes within edges such as front propagation given by a nonlinear reaction-diffusion process. In the case of intercellular transport within an axon, assuming that there is a pool of proteins that can interact autocatalytically with the population of toxic proteins, a front of toxic proteins traveling along the axon will develop. Further, we assume that the total process of invasion takes place over a time scale of about 30 years. Therefore, for a given toxic seed concentration, the parameter ρ is calibrated so that the toxic protein biomarker reaches about half its maximal value at $T = 15$ years. The weighted adjacency matrix and side view of the 83-node brain connectome are given in Fig. S1.

S2. RELATIONSHIP BETWEEN THE SOURCE POSITION AND EARLY ONSET

It is usually accepted in the medical literature that the seeding position for toxic tau-proteins is the entorhinal cortex. This location corresponds to a single node in the connectome. A key question is to understand how the disease propagates and which regions are first altered. Both pathophysiological observations and observation of amnestic syndrome in the early stages of the diseases point to the fact that nearby regions such as the hippocampal and parahippocampal regions are affected [1]. This early staging is consistent with the model. For early times, the level of toxic proteins is small and the Fisher–KPP equation

$$\dot{c}_k = -\sum_{j=1}^{N} L_{kj} c_j + \alpha c_k(1 - c_k), \qquad k = 1, \dots, N, \tag{S2}$$

is well approximated by its linearization

$$\dot{c}_k = -\sum_{j=1}^{N} L_{kj} c_j + \alpha c_k = \left(-L + \alpha \mathbb{1}\right)_{jk} c_k, \qquad k = 1, \dots, N. \tag{S3}$$

This is now a linear system of ordinary differential equations (ODEs) with constant coefficients that can be solved explicitly [2]. Let $\mathbf{c} = (c_1, c_2, \dots, c_N)^{\mathrm{T}}$ be the column vector of concentration. Then, this system can be written compactly as

$$\dot{\mathbf{c}} = M\mathbf{c}, \tag{S4}$$

where $M = -L + \alpha\mathbb{1}$. Its solution for the initial value $\mathbf{c}_0 = \mathbf{c}(T = 0)$ is

$$\mathbf{c} = \exp(TM)\mathbf{c}_0, \tag{S5}$$

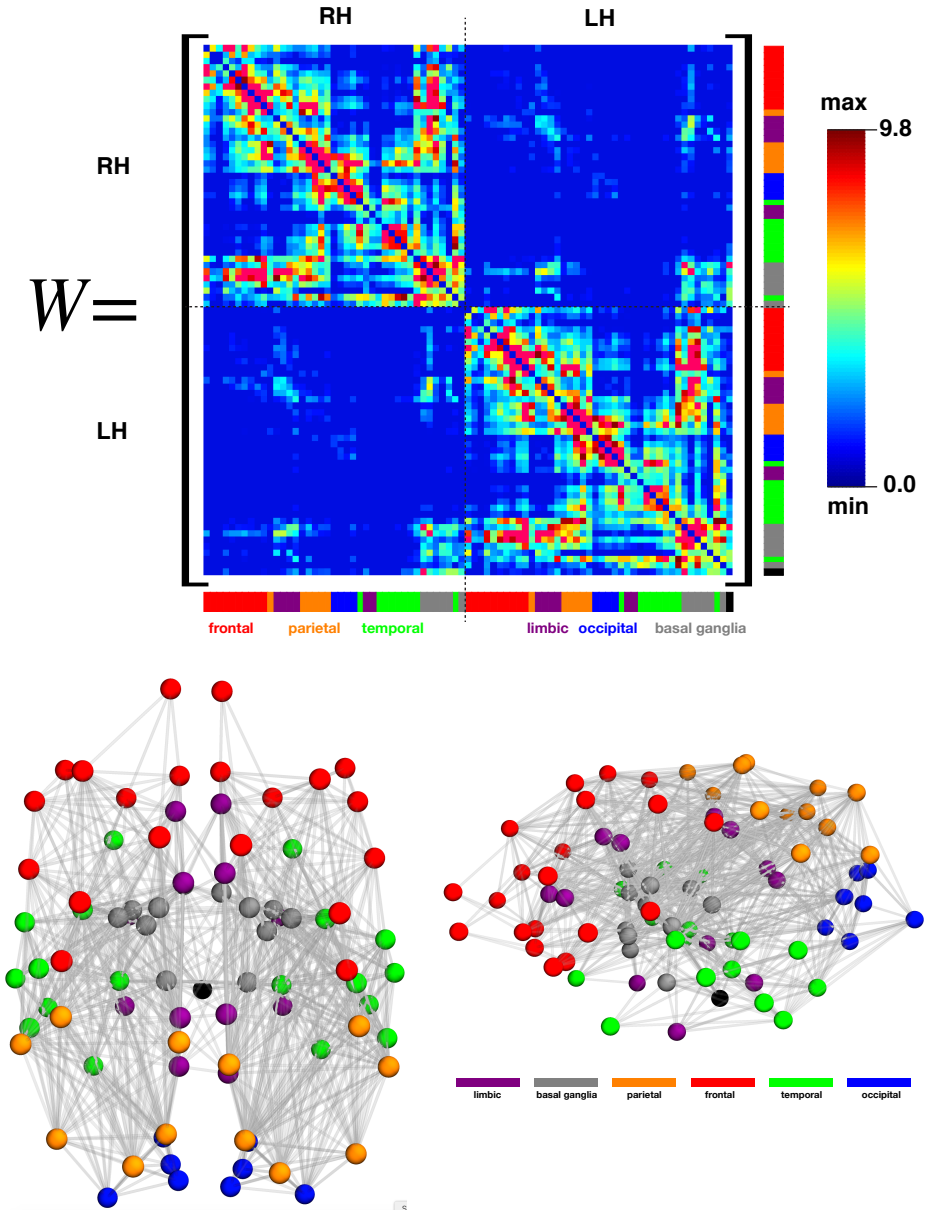

FIG. S1. The weighted adjacency matrix for the 83 connectome. The elements of this matrix are given by the ratio (number of fibers between nodes)/(length between node). They range from 0 (blue) to 9.8 (red). RH and NH denote the right and left hemispheres, respectively. The different regions and their color coding are also given

where the matrix exponential is defined, as usual, through its series $\exp(TM) = \sum_{j=0}^{\infty} T^j M^j / j!$.

Now, consider an initial condition with a seed at node k and 0 everywhere else ($c_k(T=0) = c_0, c_j(T=0) = 0, \forall j \neq k$) which we write $\mathbf{c}_0 = c_0 \mathbf{1}_k$. An important property of the graph Laplacian is that the entries of the vector $L\mathbf{1}_k$ vanish everywhere except at the entries j corresponding to nodes that are neighbors of node k. Iterating this process, we find that $L^n \mathbf{1}_k$ vanishes everywhere except at the entries j corresponding to nodes whose path length to node k is less or equal to n (the *path length* is understood here as the integer number giving the shortest number of steps or edges between two nodes, not the Euclidean distance used in weighing the adjacency matrix). This property is also true for the matrix $M = -L + \alpha \mathbb{1}$ and $M^n \mathbf{1}_k$ vanishes everywhere except at entries j corresponding to nodes whose shortest path length to node k is less or equal to n. Defining m_{jk} to be the path length between nodes j and k, for a single source at node k, we have

$$\mathbf{c} = c_0 \sum_{j=0}^{\infty} \frac{T^j}{j!} M^j \mathbf{1}_k, \tag{S6}$$

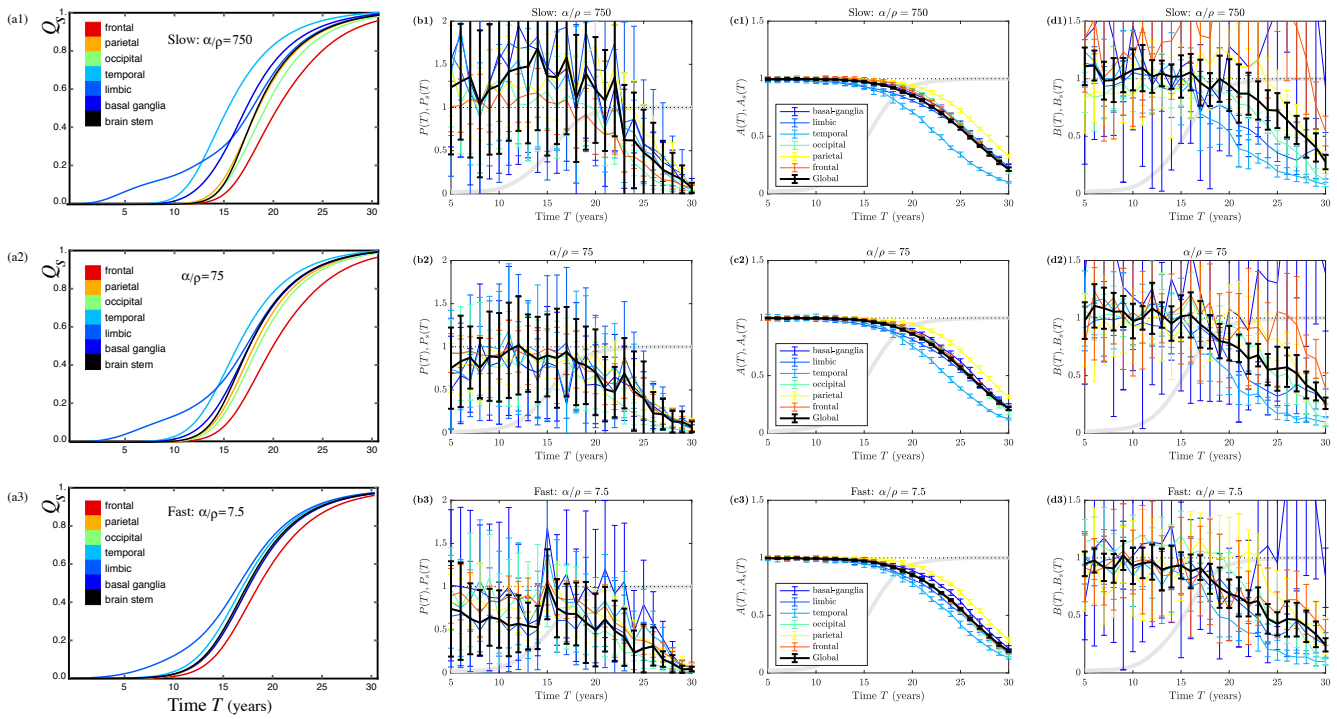

FIG. S2. Parametric study for different values of the ratio α/ρ for the network evolution and the resting state dynamics. Here, $\beta = 1/4$, $\gamma = 1/8$ for all figures, specific values from top to bottom are $\alpha = 0.996, \beta = 0.0013$ (slow); $\alpha = 0.5682, \beta = 0.076$ (reference), $\alpha = 3/4, \beta = 1/100$ (fast). The middle row corresponds to the parameter values in the main text.

which for small time can be written explicitly as

$$c_j = c_0 T^{m_{jk}} M^{m_{jk}} \mathbf{1}_k + \mathcal{O}(T^{m_{jk}+1}). \tag{S7}$$

This expression shows that at early times, to order $\mathcal{O}(T)$, the concentration at the seeded node and its neighbor increases linearly but second neighbors will only increase quadratically. This topological property of early times dynamics explains the early staging patterns observed in the disease including propagation in the hippocampal and parahippocampal regions and the temporal lobe.

S3. PARAMETRIC STUDY OF DISEASE EVOLUTION

The disease dynamics depends on two parameters α and ρ. Up to a scaling in time, the important parameter for the dynamics is the ratio α/ρ. The system is then rescaled uniformly in time so that the toxic protein biomarker reaches the same value at year 15 for all values of α/ρ. Fig. S2 shows the evolution of the network (Panel (a)) as well as the network dynamics of the coupled neural masses (Panels (b–d)) for the values in the main text as well as two interesting limits to the dynamics. In the first limiting case, shown in Fig. S2 top row, the diffusion is very slow and the disease first develops locally before propagating to other nodes. The second limit (Fig. S2 bottom row) is obtained when the diffusion is fast and the system is first seeded uniformly before amplification of the toxic seed. The intermediary case is the one studied in the main paper (Fig. S2 middle).

In the diffusion-dominated case, the damage due to the biomarkers increases uniformly. This is in contradiction to the staging behavior observed in the dynamics of these diseases where the different parts of the brain are systematically invaded over the course of the disease. In the slow case, there is very little dependence on the value of the diffusion constant. If we chose a α/ρ 10 times or 100 times larger, the dynamics is mostly unchanged as it is dominated by the exponential increase due to the linear term with coefficient α. We also see that the ordering of the regions remains unchanged. Hence, despite the fact that this ratio cannot be obtained directly from in vivo measurements or first principles, the variation of this ratio plays little role in the system as long as it is not in the diffusion dominated regime.

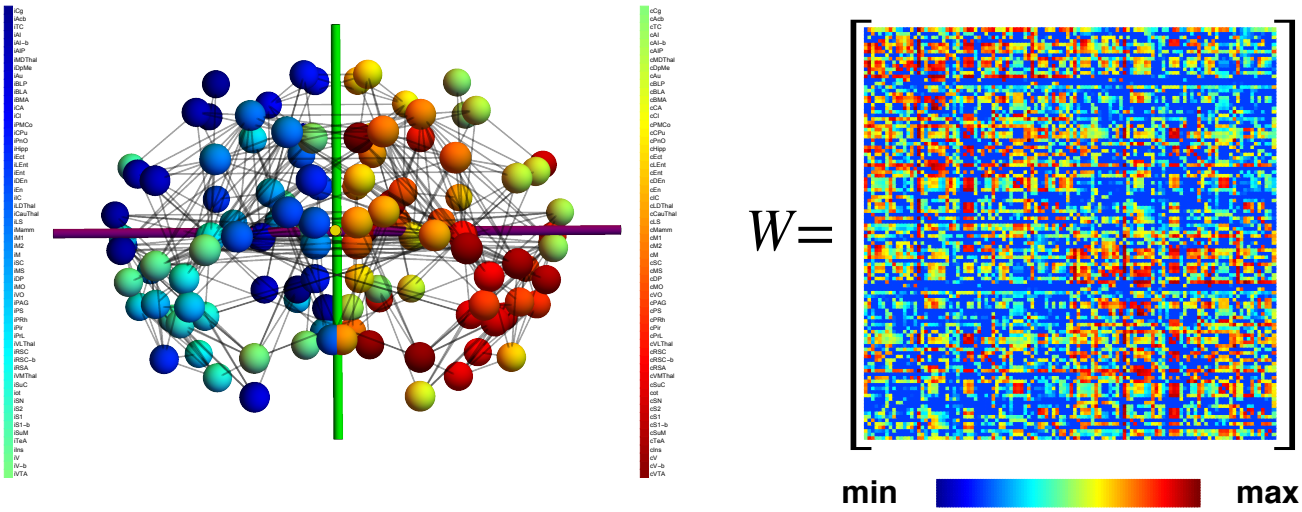

FIG. S3. The mouse connectome with $N = 116$ nodes and $M = 8642$ edges (349 strongest connection shown). Each node is associated with a brain region. The connectome and nomenclature are available from [5].

S4. THE ROLE OF ASYMMETRY

A well-known and important feature of the brain connectome is that it is a directed network. Axonal bundles have a directionality and the connections from node k to node j are, typically not the same. Hence, this asymmetry in connection leads to an asymmetry in the weighted connection matrix $\mathbf{W}$, whose coefficients w_{kj} correspond to the connection weight from node k to j. To explore the role of asymmetry, we consider a one-parameter family of connection matrices

$$\mathbf{W}^{(a)} = \mathbf{W}_{\text{sym}} + a\mathbf{W}_{\text{asym}}, \qquad a \in [-1, 1], \tag{S8}$$

where $\mathbf{W}_{\text{sym}} = (\mathbf{W} + \mathbf{W}^{\mathrm{T}})/2$ and $\mathbf{W}_{\text{asym}} = (\mathbf{W} - \mathbf{W}^{\mathrm{T}})/2$. Then, $\mathbf{W}^{(0)}$ is the symmetric part of $\mathbf{W}$, $\mathbf{W}^{(1)} = \mathbf{W}$, and $\mathbf{W}^{(-1)} = \mathbf{W}^{\mathrm{T}}$ has all connections reversed. Since $\mathbf{W}$ represents the number of connection between different nodes, the sum of all elements of $\mathbf{W}^{(a)}$ is independent of a for $a \in [-1, 1]$ and therefore represents connectomes with the same number of fibers. Given a weighted connection matrix $\mathbf{W}^{(a)}$, the graph Laplacian is

$$\mathbf{L}_a = \rho\Big(\mathbf{D}^{(a)} - \big(\mathbf{W}^{(a)}\big)^{\mathrm{T}}\Big), \tag{S9}$$

where $\mathbf{D}^{(a)}$ is the out-diagonal matrix with $d^{(a)}_{kk} = \sum_{j=1}^{N} w^{(a)}_{kj}$ and ρ is an overall velocity constant defining the time-scale of transport. In a diffusion process of the form $\dot{\mathbf{x}} = -\mathbf{L}^{(a)}\mathbf{x}$, where $\mathbf{x}$ is a vector of concentration, this choice of graph Laplacian has the desired feature that it preserves mass between nodes of equal volume ($\sum \dot{x}_i = 0$). The corresponding Fisher–KPP equation for the transport and increase in toxic proteins is given by

$$\dot{c}_k = -\sum_{j=1}^{N} L^{(a)}_{kj} c_j + \alpha c_k(1 - c_k), \qquad k = 1, \ldots, N. \tag{S10}$$

Unfortunately, there is no available directed human connectome suitable for the study of the role of asymmetric connection. However, there is a directed mesoscale mouse connectome [3] that has been used in studies of protein transport relevant to neurodegenerative diseases [4, 5]. Here, we use the weighted asymmetric connectivity matrix given in [5] containing 116 nodes and 8642 edges. We scale each entry by the length between nodes (also given in [5]) and normalise by an overall constant so that the sum of all entries is one. The resulting connectome is shown in Fig. S3.

To study the role of asymmetry, we compare the evolution of toxic proteins in the asymmetric connectome $\mathbf{W}^{(1)}$, with the reverse connectome $\mathbf{W}^{(-1)}$, and the symmetrised one $\mathbf{W}^{(0)}$ in Fig. S4A (without an evolution of the connection weights in order to isolate the effect of asymmetry). We seed toxic protein at the ispilateral and contraletral caudoputamen as it was found to be the most likely place for seeding [5]. The parameter ρ is chosen so that the concentration of toxic proteins $C^{(a)}(15) = 1/2$ for the asymmetric connectome in arbitrary time units. We see that the asymmetric version of the connectome delays considerably disease progression by as much as 6 time units. In Fig. S4B, we compute the time T^* at which $C^{(a)}(T^*) = 1/2$ and show

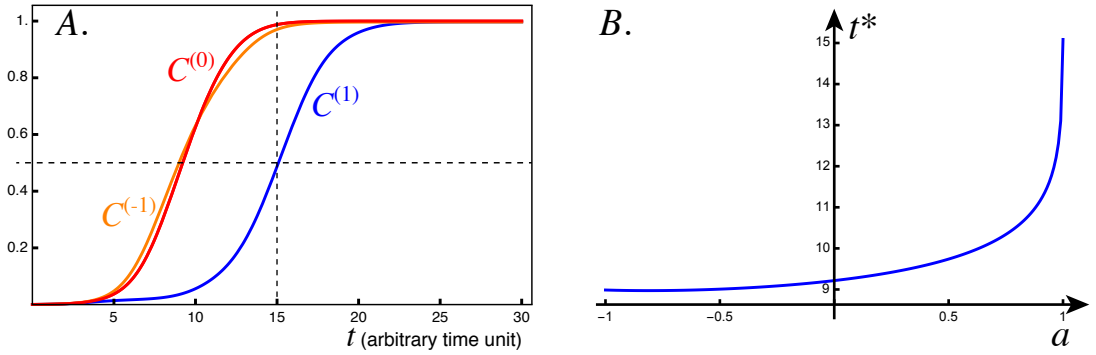

FIG. S4. The role of asymmetry in the propagation of the concentration $C^{(a)}(T)$ of toxic protein. Here, $\alpha = 1$, $\rho = 4$ and $c_{16}(0) = c_{74}(0) = 0.025$.

α	reaction	0.75years^{-1}
ρ	diffusion	0.01mm/years
β	damage	0.25years^{-1}
γ	axonopathy	0.125years^{-1}
λ	Hopf decay parameter	-0.01s^{-1}
ω	average intrinsic frequency	40s^{-1}
κ	coupling gain	10
t_{sim}	resting-state simulation time	10s

TABLE S1. Main simulation parameters. The parameters chosen for the degeneration dynamics are taken from [6] based on [7] and [8]. For the neural mass model, the parameters are adapted from [9].

the systematic delay due to the particular asymmetry found in the mouse connectome. However, apart from this delay, the propagation of the biomarker proceeds without much difference and saturate at the same level (note that for a directed graph this is not a general property of the equation since the equilibrium state is not homogeneous).

S5. SOLVING THE NEURONAL MASS MODEL

Define the sigmoidal function $S(x) = 1/(1+\exp(-x))$ and let $F(z_k) = z\big(\lambda + i\omega_k - \big|z_k^2\big|\big)$ with $i = \sqrt{-1}$. To assess resting state neural dynamics for a given weighted connectivity matrix $\mathbf{W} = (w_{kj})$, we solved the delay differential equation

$$\dot{z}_k = F(z_k) + \kappa S\left(\text{Re}\left(\sum_{j=1}^{N} w_{kj} z_j(t-\tau_{kj})\right)\right), \tag{S11}$$

with decay parameter λ, intrinsic frequencies $\omega_k = \omega + \delta_k$, and overall connection strength κ. The deviations δ_k were sampled from a normal distribution with mean zero and variance 0.1Hz. The delays τ_{kj} were chosen proportional to the distance d_{kj} between node k and j from the connectome data, $\tau_{kj} = d_{kj}/150$, to correspond to a transmission speed of 150cm/s. The delays were then discretized to have a maximum of 40 distinct delays. Table S1 summarizes the parameter values and, for completeness, the matrices of connection weights $\mathbf{W} = (w_{kj})$ (before disease evolution) and discretized delays (τ_{kj}) are available as supplemental files. We integrated the resulting system of equations using MATLAB's `dde32` routine with default settings and error tolerances: We chose random initial conditions (and constant history), discarded a transient of $t_{\text{trans}} = 3$s, and then calculated the dynamics of (S11) for t_{sim}s of resting state dynamics.

[1] J. P. Kesslak, O. Nalcioglu, and C. W. Cotman, Neurology **41**, 51 (1991).
[2] A. Goriely, *Integrability and Nonintegrability of Dynamical Systems* (World Scientific Publishing Company, 2001).
[3] S. W. Oh, J. A. Harris, L. Ng, B. Winslow, N. Cain, S. Mihalas, Q. Wang, C. Lau, L. Kuan, A. M. Henry, *et al.*, Nature **508**, 207 (2014).
[4] M. X. Henderson, S. Sedor, I. McGeary, E. J. Cornblath, C. Peng, D. M. Riddle, H. L. Li, B. Zhang, H. J. Brown, M. F. Olufemi, *et al.*, Neuron **105**, 1 (2020).

[5] M. X. Henderson, E. J. Cornblath, A. Darwich, B. Zhang, H. Brown, R. J. Gathagan, R. M. Sandler, D. S. Bassett, J. Q. Trojanowski, and V. M. Lee, Nat Neurosci **22**, 1248 (2019).
[6] S. Fornari, A. Schäfer, A. Goriely, and E. Kuhl, J R Soc Interface **16**, 20190356 (2019).
[7] F. Kundel, L. Hong, B. Falcon, W. A. McEwan, T. C. Michaels, G. Meisl, N. Esteras, A. Y. Abramov, T. J. Knowles, M. Goedert, *et al.*, ACS chemical neuroscience **9**, 1276 (2018).
[8] S. Fornari, A. Schäfer, E. Kuhl, and A. Goriely, J Theor Biol **486**, 110102 (2020).
[9] G. Deco, V. Jirsa, A. R. McIntosh, O. Sporns, and R. Kötter, Proc Nat Acad Sci USA **106**, 10302 (2009).